

Subject-specific identification of three dimensional foot shape deviations using statistical shape analysis

Stanković, Kristina ; Huysmans, Toon; Danckaers, Femke ; Sijbers, Jan; Booth, Brian G.

DOI

[10.1016/j.eswa.2020.113372](https://doi.org/10.1016/j.eswa.2020.113372)

Publication date

2020

Document Version

Final published version

Published in

Expert Systems with Applications

Citation (APA)

Stanković, K., Huysmans, T., Danckaers, F., Sijbers, J., & Booth, B. G. (2020). Subject-specific identification of three dimensional foot shape deviations using statistical shape analysis. *Expert Systems with Applications*, 151, Article 113372. <https://doi.org/10.1016/j.eswa.2020.113372>

Important note

To cite this publication, please use the final published version (if applicable). Please check the document version above.

Copyright

Other than for strictly personal use, it is not permitted to download, forward or distribute the text or part of it, without the consent of the author(s) and/or copyright holder(s), unless the work is under an open content license such as Creative Commons.

Takedown policy

Please contact us and provide details if you believe this document breaches copyrights. We will remove access to the work immediately and investigate your claim.



Subject-specific identification of three dimensional foot shape deviations using statistical shape analysis

Kristina Stanković^{a,*}, Toon Huysmans^{a,b}, Femke Danckaers^a, Jan Sijbers^a, Brian G. Booth^a

^aimec - Vision Lab, Department of Physics, University of Antwerp, Antwerp, Belgium

^bSection on Applied Ergonomics & Design, Department of Industrial Design, Delft University of Technology, CE Delft, the Netherlands

ARTICLE INFO

Article history:

Received 23 April 2019

Revised 3 December 2019

Accepted 9 March 2020

Available online 14 March 2020

Keywords:

3D foot scans

Statistical shape modelling

Personalized medicine

Outlier detection

ABSTRACT

The high prevalence of foot pain, and its relation to foot shape, indicates the need for an expert system to identify foot shape abnormalities. Yet, to date, no such expert system exists that examines the full 3D foot shape and produces an intuitive explanation of why a foot is abnormal. In this work, we present the first such expert system that satisfies those goals. The system is based on the concept of model-based outlier detection: a statistical shape model (SSM) is generated from 186 3D optical foot scans of healthy feet. This model acts as a knowledge base which is then parameterized by one's demographic characteristics (e.g., age, weight, height, shoe size) through a multivariate regression. This regression introduces model flexibility as it allows the model to be fine tuned to a specific individual. This fine tuned model is then used as a baseline to which the individual's 3D foot scan can be compared using standard statistical tests (e.g. t-tests). These statistical tests are performed at each vertex along the foot surface to identify the degree and location of shape outliers. Our expert system was validated on foot scans from patients with hallux valgus and abnormal foot arches. As expected, our results varied per patient, confirming that feet with the same clinical classification still show high shape variability. Additionally, the foot shape abnormalities identified by our system not only agreed with the expected location and severity of the tested foot deformities, but our analysis of the full 3D foot shape was able to completely characterize the extent of those abnormalities for the first time. These results show that the combination of statistical shape modelling, multivariate regression, and statistical testing is powerful enough to perform outlier detection for 3D foot shapes. The resulting insights provided by this system could prove useful in both shoe design and clinical diagnosis.

© 2020 Elsevier Ltd. All rights reserved.

1. Introduction

It is estimated that anywhere between 17 and 41% of the general population experience foot pain and, in roughly half of these cases, the foot pain is disabling (Garrow, Silman, & Macfarlane, 2004; Hawke & Burns, 2009; Hill, Gill, Menz, & Taylor, 2008). For some people, this pain is linked to foot deformities, with common conditions including hallux valgus (Garrow et al., 2001; Nix, Vicenzino, Collins, & Smith, 2012), collapsed foot arches (Xiong, Goonetilleke, Witana, Weerasinghe, & Au, 2010; Young, Niedfeldt, Morris, & Eerkes, 2005), and club feet (Agarwal & Rastogi, 2018; Ganesan, Luximon, Al-Jumaily, Balasankar, & Naik, 2017). For others, foot pain has been associated with improperly fitting footwear

(de Castro, Rebelatto, & Aurichio, 2010; Dobson, Riddiford-Harland, Bell, & Steele, 2018), indicating that a more precise characterization of foot shape would be valuable in footwear fitting and design (Deselnicu, Vasilescu, Mihai, Purcarea, & Militaru, 2016; Rodrigo, Goonetilleke, & Witana, 2012; Sarghie, Mihai, & Herghiligiu, 2016; Wunderlich & Cavanagh, 1999). Despite a clear link between foot shape and foot pain, one study has reported that more than half of its participants who experienced debilitating foot pain did not seek professional help (Garrow et al., 2004). These results suggest that either foot shape abnormalities are difficult for a non-expert to assess, or that access to professional foot care is limited. Either way, this indicates a need for an expert system that can assess whether one's foot shape is abnormal or not. Such a system could reduce one's future foot pain by either identifying foot deformities requiring professional care, or by recommending better footwear choices (Dohi, Mochimaru, & Kouchi, 2001; Hawes et al., 1994; Mochimaru, Kouchi, & Dohi, 2000; Nigg, Nurse, & Stehanyshyn, 1999).

* Corresponding author.

E-mail addresses: kristina.stankovic@uantwerpen.be (K. Stanković), t.huysmans@tudelft.nl (T. Huysmans), femke.danckaers@uantwerpen.be (F. Danckaers), jan.sijbers@uantwerpen.be (J. Sijbers), brian.booth@uantwerpen.be (B.G. Booth).

The development of expert systems for foot assessment remains an open research question. Traditionally, experts such as physical therapists and podiatrists have classified feet based on visual appraisal (Dahle, Mueller, Delitto, & Diamond, 1991; Garrow et al., 2001; Menz, Fotoohabadi, Wee, & Spink, 2012), with foot arch heights, ankle bone curvatures, and toe angles being key shape cues (Garrow et al., 2001; Redmond, Crane, & Menz, 2008; Young et al., 2005). Unfortunately, these visual appraisals introduce a measure of subjectivity into the analysis of foot shape, resulting in examinations that can vary significantly between clinicians (Knippels et al., 2014).

In recent years, attempts have been made to develop expert systems based on objective measures of foot shape, most notably in the form of outlier detection algorithms (Z. Yuan, 2018). These include the arch index measure introduced by Cavanagh and Rodgers (1987). Using measurements from 2D footprints and statistical thresholds, arch index can classify feet as being high-, normal-, or flat-arched. Similar statistical thresholds have also been applied to 1D arch height measures (Nigg, Cole, & Nachbauer, 1993), center of pressure trajectories (Song, Hillstrom, Secord, & Levitt, 1996), and forefoot-rearfoot angles (Freychat, Belli, Carret, & Lacour, 1996) in order to identify abnormal arch heights. A full review of such techniques can be found in the work of Xiong et al. (2010). Similar statistical thresholds have also been defined for hallux valgus based on the hallux abductus angle (Chen, Zhou, Hlavacek, & Xu, 2013; Piqué-Vidal & Vila, 2009), and for club feet based on calcaneus distances (Agarwal & Rastogi, 2018). These approaches can be thought of as expert systems where the user inputs a given foot measurement or footprint, the knowledge base is a statistical model, and the inference engine performs outlier detection using significance thresholds. Other expert systems also exist for foot assessment, but they do not consider foot shape (Barton & Lees, 1995; Naser & Mahdi, 2016; Piecha, 2000).

Despite the benefits these objective techniques provide, they also have their limitations. Many studies are based purely on scalar measurements or 2D images of the foot (e.g. footprints) instead of the full 3D foot shape (Cavanagh et al., 1997; Cavanagh & Rodgers, 1987). It has been shown that the full 3D foot shape is not only important for footwear design (Goonetilleke, 1997; Mauch, Grau, Krauss, Maiwald, & Horstmann, 2009; Mochimaru et al., 2000; Nix et al., 2012), but it also cannot be fully recovered from lower-dimensional foot measurements (Xiong, Goonetilleke, Witana, & Lee Au, 2008). As a result, these expert systems do not provide a complete assessment of foot shape.

Additionally, existing expert systems for foot shape provide only coarse groupings, usually only identifying if a foot is normal or abnormal. Several studies (Anderson, Blais, & Green, 1956; Debrunner, 1965; Kouchi, 1998) reported inter-individual differences for width and height measures of feet within the same class, such as foot size classes. Similarly, different degrees of hallux valgus deformity and toe deformities were associated with different shoe needs (Menz & Morris, 2005). These results suggest that foot shapes within the same class can still vary significantly and that this variance should be further considered in an expert system.

We propose that an expert system for foot shape analysis should ideally satisfy four criteria. First, the system's knowledge base should contain information on the full 3D foot shape and not simply 2D or 1D foot measurements. This criterion would ensure that assessment of the complete foot is possible. Second, the system's inference engine should provide more than simply a label of whether a foot is normal or not. If a foot is labelled as abnormally-shaped, the system should explain what part of the foot is abnormal and to what extent it is abnormal. Third, the system's user interface should be simple enough for a non-expert to use. This criterion aims to eliminate the subjectivity seen in visual assessments as well as ensuring that access to the system is not limited

by access to a foot care professional. Finally, the system should employ methods that are familiar to foot care professionals, thereby ensuring that they can confidently recommend such a system and properly follow-up on the system's results.

To address these criteria, we introduce an expert system based on the concepts of outlier detection for the assessment of one's full 3D foot shape. The user interface requires one to simply enter a 3D optical scan of their foot and basic demographic information (e.g. age, weight, shoe size), making the system usable by a non-expert. The knowledge base of the system is centered on the statistical shape modelling, a technique that has shown to be a useful tool in a variety of applications (Ahmad, Taylor, Lanitis, & Cootes, 1997; Costafreda et al., 2011; Ferrari, Jurie, & Schmid, 2007; 2010; Shen et al., 2012; Zhang, Gao, Gao, Munsell, & Shen, 2016). The model is constructed from healthy individuals and a regression analysis, like those in Klein, Hu, Reed, Hoff, and Rupp (2015); Wang et al. (2016), is used to link the user-entered demographic information to a baseline foot shape measurement. Finally, statistical testing is employed to compare one's measurement to this statistical baseline. This testing is performed across the foot surface in order to identify the location and extent of shape abnormalities (Bazarian, Zhu, Blyth, Borrino, & Zhong, 2012; Booth et al., 2016; Harris et al., 2013; Khanduja et al., 2016).

Our proposed expert system merges together established shape analysis and outlier detection techniques, thereby making it a natural extension to methods currently used by foot care professionals. We hypothesize the use of such techniques can provide sufficient analytical power to become the first expert system to simultaneously satisfy the four criteria mentioned earlier.

2. Methods

Our proposed expert system for foot shape assessment consists of two main parts: the building of a statistical shape model (i.e. the knowledge base), and the comparison of an individual's foot to that model (i.e. the inference engine). In both parts of the system, we represent a foot shape, \mathbf{X} , as a triangulated 3D mesh of the foot surface. Also, let $\{\mathbf{X}_1, \mathbf{X}_2, \dots, \mathbf{X}_N\}$ be the N foot scans from which a statistical shape model will be computed.

In order to perform meaningful statistics on such a shape representation, an anatomical correspondence needs to be established between all N foot meshes and these meshes have to be spatially aligned. In Section 2.1, the correspondence and alignment procedure is explained after which the model building and personalized analysis parts of our pipeline are presented in Sections 2.2 and 2.3, respectively.

2.1. Correspondence establishment and anatomical alignment

Initially, each 3D foot mesh has a different number and order of vertices. These meshes can also vary in their position within the field of view of the 3D scanner. In order to analyze the shapes represented in 3D foot meshes, we must first ensure that each mesh has the same vertices located in the same anatomical locations. Second, we must then align the 3D foot meshes to remove the influence of pose on the analysis of shape. The first procedure is referred to as shape correspondence while the second is referred to as anatomical alignment. Fig. 1 shows the effect of these procedures on two randomly-chosen feet.

2.1.1. Shape correspondence

To bring two 3D foot meshes into anatomical correspondence, we employ the pairwise registration of Danckaers et al. (2014). To do so, we choose one foot mesh, \mathbf{X}_{ref} , as our reference foot mesh and deform it to match the other foot meshes in our analysis. At a

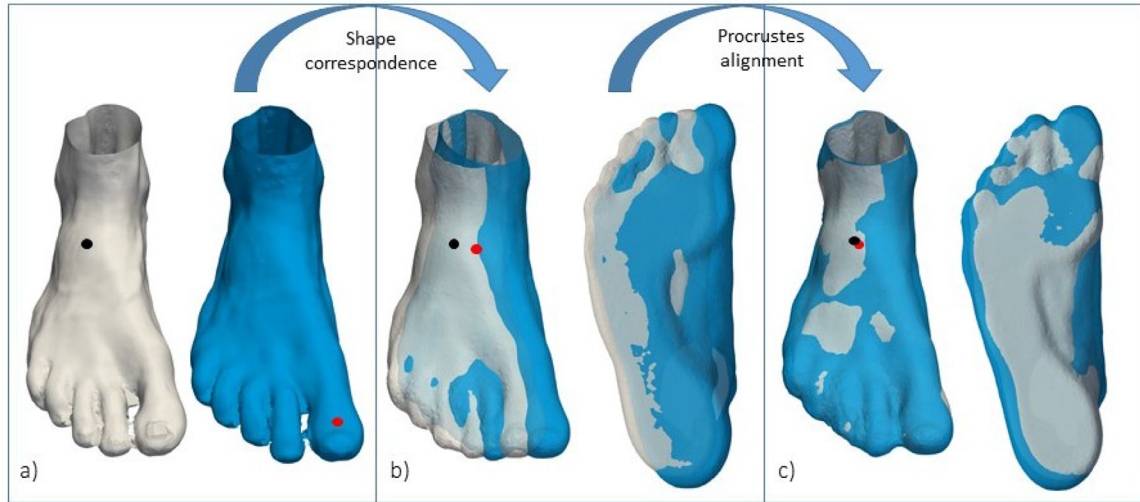


Fig. 1. Correspondence establishment and alignment. a) Two randomly chosen feet with unmatched vertices before correspondence establishment, b) overlapped feet after correspondence establishment, c) overlapped feet after anatomical alignment.

high level, this deformation is described by

$$\mathbf{X}_{target} = \Psi(T(\mathbf{X}_{ref}, \beta)), \quad (1)$$

where \mathbf{X}_{target} is a foot mesh being analyzed, T is an affine transformation and Ψ is a set of displacement vectors. The degree of the deformation operation is controlled by a user-defined elasticity parameter, β . We solve for T and Ψ using the iterative procedure defined in Danckaers et al. (2014). Briefly, this iterative procedure operates by fixing one of the transformations (e.g. Ψ) and then solving Eq. (1) for the other transformation (e.g. T). Subsequently, the procedure solves Eq. (1) for the transformation that was fixed in the former iteration (Ψ) while now fixing the previously-computed unknown transformation (T). This process is iterated until the magnitude of the observed shape changes is below a set threshold (0.01 mm). During the iterations, the elasticity parameter, β , is increased to gradually introduce more deformation as the alignment improves. Further details can be found in Danckaers et al. (2014). The final result is the reference mesh \mathbf{X}_{ref} deformed to have its shape as similar as possible to the shape of the target mesh \mathbf{X}_{target} . At this point, \mathbf{X}_{target} is replaced by $\Psi(T(\mathbf{X}_{ref}))$, ensuring that each foot mesh has the same number of vertices ordered in the same fashion (Fig. 1b). This pairwise registration is applied for all N foot shapes in the database to make sure all shapes are in correspondence with each other.

2.1.2. Procrustes analysis

Once the N foot shapes have been brought into correspondence, their meshes need to be brought into spatial alignment before statistics can be accurately performed. We achieve this alignment through a Procrustes Analysis as presented by Stegmann and Gomez (2002). This analysis consists of three steps that estimate the translation, scale, and rotation of one shape that brings it into alignment with another (Fig. 1c). Since the foot scans are obtained in a standing position, we further constrain the translation in the vertical direction to ensure that all 3D foot meshes remain aligned to the ground plane.

For the personalized analysis step of our pipeline, a single Procrustes Analysis is sufficient to bring the individual's 3D foot mesh into alignment with the SSM. However, when building the SSM, all 3D foot meshes need to be superimposed. We accomplish this task by performing a Generalized Procrustes Analysis Stegmann and Gomez (2002). In a Generalized Procrustes Analysis, a single 3D foot mesh is chosen as a target and the remaining $N - 1$

meshes are aligned to it using the traditional Procrustes Analysis. An initial estimate of the mean shape is then obtained. This mean shape is then chosen as the target mesh and the process repeats itself until no further changes in the mean shape are seen. Further details can be found in Stegmann and Gomez (2002).

The shape correspondence and alignment procedures above are followed for each individual. In the case of the model building task, the shape correspondence is iterated together with Generalized Procrustes Alignment in order to avoid any bias from the choice of \mathbf{X}_{ref} . In each iteration, the population mean calculated from the previous iteration is used as the reference foot mesh (Stanković et al., 2016). Convergence is reached if the average distance between corresponding points on the reference mesh from the previous iteration and the reference mesh from the current iteration is less than $\varepsilon = 0.001$ mm.

2.2. Model building

From our set of N aligned 3D healthy foot scans, we built a 3D statistical shape model using Principal Component Analysis (PCA) (Stanković et al., 2018). This SSM is then combined with a multivariate linear regression to fine tune the SSM based on different covariates (such as age, shoe size, BMI, etc.). Using this fine-tuned model, a maximum-likelihood prediction of one's foot shape can be obtained. Then, residuals are calculated between these predicted surfaces and the aligned, measured, foot surfaces. These model-building steps are summarized in Fig. 2.

2.2.1. Principal component analysis

Once all foot scans have been brought into correspondence and aligned to an unbiased reference, a statistical shape model is built from the population. Let N be the number of 3D foot shapes in our healthy population, with every shape consisting of n vertices in 3D. This population is represented by $N - 1$ dimensional cloud within $3n$ -space, where each point represents a foot shape. Principal component analysis (PCA) is then used to represent this cloud by a mean shape and $N - 1$ eigenmode vectors, where the first eigenmode describes the largest variance in the population, the second eigenmode the second largest variance orthogonal to the first, etc. The resulting statistical shape model consists of the mean shape $\bar{\mathbf{x}} \in \mathbb{R}^{3n}$ and the main shape modes: the principal components (PC) $\mathbf{P} \in \mathbb{R}^{3n \times (N-1)}$. Under this PCA model representation, a new shape

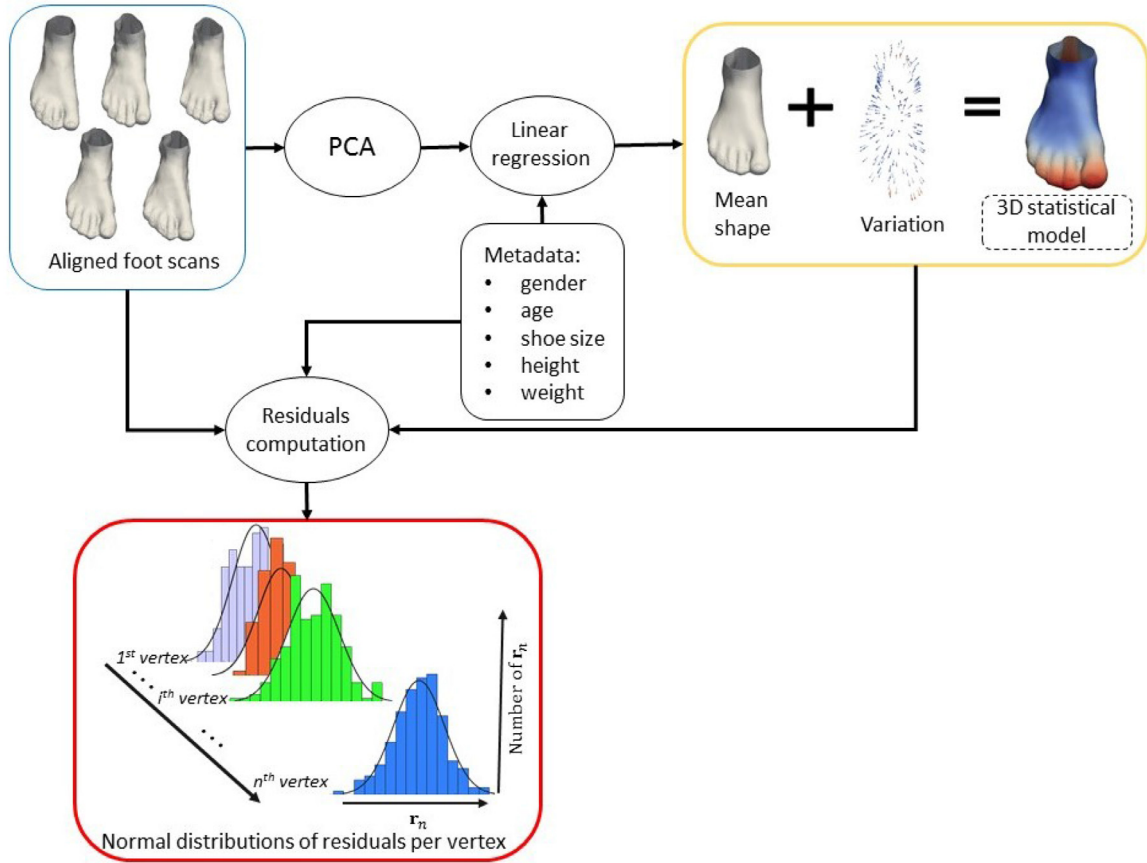


Fig. 2. Model building. a) Once all feet are brought into correspondence and aligned (blue box), a 3D foot SSM is built using Principal Component Analysis. b) Metadata is combined with the 3D SSM to develop a tunable shape model (yellow box) c) Residuals for each vertex are computed between every aligned foot and its corresponding SSM prediction (red box). (For interpretation of the references to colour in this figure legend, the reader is referred to the web version of this article.)

$\mathbf{y} \in \mathbb{R}^{3n}$ can be formed by a linear combination of the PCs:

$$\mathbf{y} = \bar{\mathbf{x}} + \mathbf{P}\mathbf{b}, \quad (2)$$

with $\mathbf{b} \in \mathbb{R}^{(N-1)}$ being the PC weight vector mapping the shape to the statistical model parameters (Shlens, 2014). In the context of our work, $\bar{\mathbf{x}}$ is the average foot shape, the principal components \mathbf{P} can be interpreted as a set of deformations, and the PC weights, \mathbf{b} , are computed to weight each deformation such that the average foot shape gets warped into the specific foot shape \mathbf{y} (see the upper-right, yellow, box in Fig. 2).

2.2.2. Incorporation of subject characteristics

While PCA allows us to build a 3D SSM, it has no natural way to handle covariates that can impact foot shape (e.g. weight, sex, shoe size). To account for these covariates, we link them to the SSM using multivariate multiple linear regression (Dattalo, 2013). Suppose we have a covariate vector $\mathbf{f} = [f_1, f_2, \dots, f_k, 1]^T \in \mathbb{R}^{k+1}$ that contains information of an individual's age, shoe size, etc. as well as a 1 at its end to allow for a constant offset in regression. We can define the relationship between this covariate vector and the PCA weight vector $\mathbf{b}_i \in \mathbb{R}^{N-1}$ of each shape \mathbf{X}_i from the dataset using a linear model. A mapping matrix $\mathbf{M} \in \mathbb{R}^{(N-1) \times (k+1)}$, describing the relationship between the PCA weight matrix $\mathbf{B} = [\mathbf{b}_1, \mathbf{b}_2, \dots, \mathbf{b}_N] \in \mathbb{R}^{(N-1) \times N}$ and the feature matrix $\mathbf{F} = [\mathbf{f}_1, \mathbf{f}_2, \dots, \mathbf{f}_N] \in \mathbb{R}^{(k+1) \times N}$ is calculated by

$$\mathbf{M} = \mathbf{B}\mathbf{F}^+, \quad (3)$$

where \mathbf{F}^+ is the pseudoinverse of \mathbf{F} (Danckaers, Huysmans, Lacko, & Sijbers, 2015). With this mapping matrix, a new PC weight vector

\mathbf{b} can be generated from given features \mathbf{f} as follows:

$$\mathbf{b} = \mathbf{M}\mathbf{f}. \quad (4)$$

Through this linear regression, we link the shape deformations represented by the principal components \mathbf{P} to the demographic characteristics of the individual. In this way, the matrix \mathbf{M} effectively captures how much each demographic feature influences the foot shape. By substituting Eq. (4) into Eq. (2), we obtain the statistical shape model which incorporates the shape variation influenced by an individual's covariates:

$$\mathbf{y} = \bar{\mathbf{x}} + \mathbf{P}\mathbf{M}\mathbf{f}. \quad (5)$$

By providing an individual's demographic characteristics, the most plausible corresponding healthy foot shape can then be simulated using Eq. (5).

2.2.3. Residual calculation

Our SSM defined by Eq. (5) provides us with a model of the foot shape as a whole. To further localize our subsequent analysis, we augment our SSM with residual distributions at each mesh vertex. For each 3D mesh used in building our model, we calculated residuals between it and the corresponding foot shape prediction given by Eq. (5). Each vertex thus obtains the residual vector \mathbf{r} :

$$\mathbf{r} = \mathbf{v}_r - \mathbf{v}_p, \quad (6)$$

where \mathbf{v}_r is the vertex of the measured foot mesh and \mathbf{v}_p is the corresponding vertex of the predicted foot mesh.

Since the variations in vertex position along tangential directions do not induce shape variations, and since we are only interested in shape variations, we further restrict our analysis to varia-

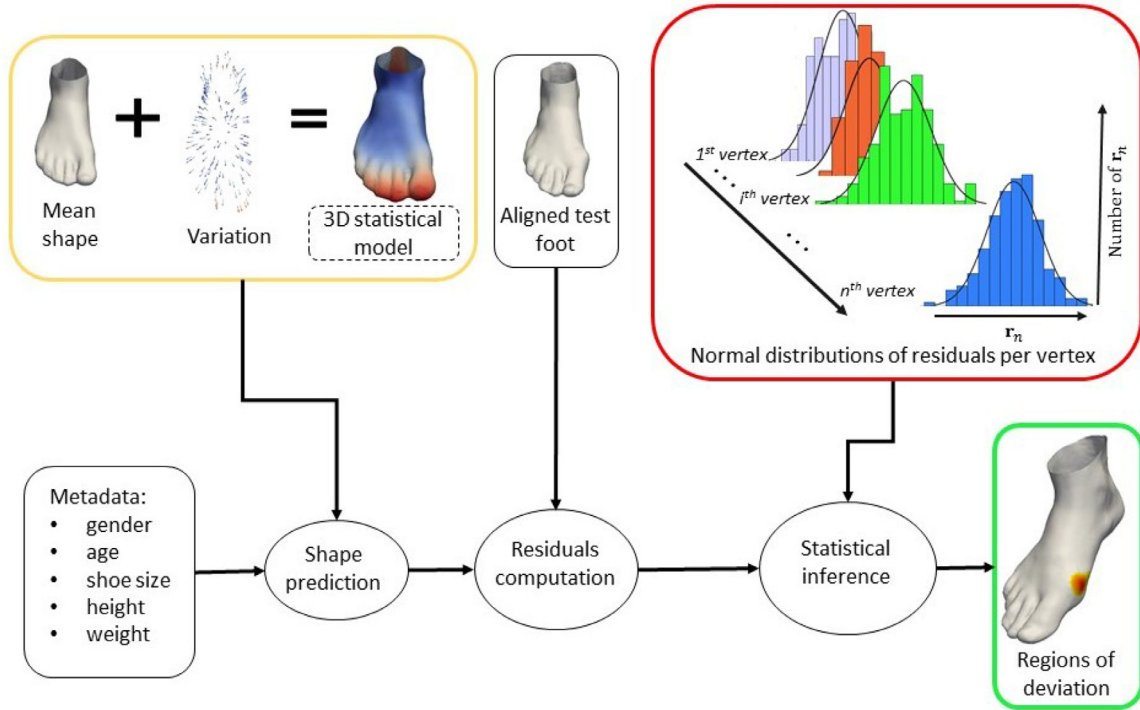


Fig. 3. Procedure for the personalized analysis of an individual's foot shape. a) The predicted healthy shape for the individual's foot is obtained using the SSM from the model-building (yellow box) and metadata of the individual b) Residuals for each vertex are computed between the aligned, measured foot shape and its corresponding prediction c) Calculated residuals are compared to residuals obtained in the model-building (red box) using statistical significance tests (green box). (For interpretation of the references to colour in this figure legend, the reader is referred to the web version of this article.)

tions in vertex position along the direction normal to the foot surface. For this reason, the vector \mathbf{r} is projected onto the vertex normal \mathbf{n}_p of the predicted foot mesh as follows:

$$r_n = \mathbf{r} \cdot \mathbf{n}_p. \quad (7)$$

where r_n is the normal component of \mathbf{r} (Glassner, 1994; Henri, 1971).

Residuals are calculated using Eq. (7) for each vertex of each 3D mesh used in the model-building procedure. Normal distributions are then fit to the residuals at each vertex to summarize local shape variations that are not otherwise captured by the SSM.

2.3. Personalized foot shape analysis

To evaluate the 3D foot shape of a new individual, we detect shape anomalies based on the 3D foot SSM built earlier (Fig. 2). To do this, we first predict the healthy foot shape of the new individual using Eq. (5). Then, we establish a correspondence between the predicted foot shape and the individual's foot shape using the algorithm described in Eq. (1). The individual's foot mesh is then brought into alignment with the predicted foot mesh using the Procrustes alignment algorithm described earlier. Finally, we compute, and statistically test, residuals between the aligned mesh and the predicted mesh as described below. The full procedure is displayed in Fig. 3.

2.3.1. Statistical inference

To identify outliers in 3D foot shape, we performed single-sample t -tests for each residual projection of the test mesh. To achieve this, we computed the residual between each vertex on the individual's aligned foot mesh and its corresponding predicted mesh using Eq. (6). Since we are interested in variations present in the mesh along the direction normal to the foot surface, we pro-

jected vector \mathbf{r} onto the surface normal using Eq. (7). Finally, we tested whether there was a significant difference ($p < 0.05$) for this individual's shape residuals by comparing them to the corresponding Normal distributions generated in the model-building. We conducted multiple comparisons correction with False Discovery Rate (FDR) for a given threshold $\alpha = 0.05$ (Storey, 2011).

3. Experiments

3.1. Dataset

To evaluate our shape analysis technique, we collected 3D optical scans of the feet of 204 Belgian adults: 132 men and 72 women. Participation in the study was entirely voluntary and demographic information (age, BMI, height, weight, and shoe size) was collected for the whole cohort (Table 1). All factors except shoe size were self-reported, while shoe size was measured using a Brannock device. Additional factors such as race and ethnicity were not noted. The Ethics Committee of the Antwerp University Hospital approved the study and all subjects gave their written informed consent before participating.

The 3D optical scans of the participant's feet were acquired with an Elinvision Tiger 3D laser scanner (rs scan, Paal, Belgium). The accuracy of the 3D scanner was 0.3 mm. A total of two scans were made per person: one of the left foot and one of the right foot. Both left and right feet were scanned while standing in a relaxed pose on both feet. Prior to the analysis, the scans of left feet were flipped along the medial-lateral axis so as to orient them in the same fashion as the right feet. Also, all 3D scans were cropped 2.0 cm above the average of the lateral and medial malleolus to decrease the effect of different lower leg poses on subsequent analysis. The obtained 3D meshes were used for further analysis.

Table 1
Metadata for the whole cohort, divided between the model-building and testing phases.

		Age [years]	Shoe size [European (Mondopoint)]	Weight [kg]	Height [cm]	BMI [$\frac{kg}{m^2}$]
Model-building phase	μ	36.5	41.7(265/101)	72.6	176.0	23.4
	σ	12.5	2.8(18.3/7.1)	11.4	8.3	3.1
	min	18	36.0(225/90)	49.0	150.0	17.9
33 females & 60 males	max	62	47.0(300/114)	100.0	196.0	32.7
Test phase	μ	43.0	41.4(263/100)	77.3	174.8	25.2
	σ	12.8	2.5(18/7)	15.1	9.1	4.3
	min	19	36.0(225/90)	47.0	156.0	18.4
39 females & 72 males	max	68	47.5(304/116)	144.0	198.0	41.6

Table 2
Exclusion and inclusion criteria for each group as well as the number of 3D foot meshes used for model-building and testing phases.

	AI	HAA	Number of individuals/ feet (training)	Number of individuals/ feet (testing)	Total number of individuals/feet
High arch	< 0.24	< 14°	0/0	21/40	21/40
Flat arch	> 0.33	< 14°	0/0	26/40	26/40
Normal arch	[0.24,0.33]	< 14°	93/186	34/40	127/226
Hallux valgus	any	> 14°	0/0	30/46	30/46

The number of feet is not always equal to twice the number of individuals, due to differences in AI and HAA between left and right feet.

3.2. Inclusion-exclusion criteria

For evaluation purposes, all individuals were categorized into one of four groups: healthy individuals with a normal foot arch, healthy individuals with a high foot arch, healthy individuals with flat feet, and individuals with hallux valgus. Each of these four groups are described further in Table 2. Individuals were considered healthy if they had no foot or leg complaints at the time of measurement. For the individuals with hallux valgus, we measured the hallux abductus angle (HAA) of each individual using the 3D anatomical annotation approach described in Chen et al. (2013). A foot is considered as having a hallux valgus if its HAA is larger than 14 degrees, a threshold which is in line with the previous study of Menz and Morris (2005). These feet were also assessed using the Manchester Scale (Garrow et al., 2001), with the majority of cases being scored as of mild (45.65%) or moderate (47.8%). Only a few severe hallux valgus cases were present (6.55%).

To classify individuals based on their foot arch height, we employed the standard approach of thresholding based on the arch index measure of Cavanagh and Rodgers (1987). This measure was applied to plantar pressure measurements taken from each participant as they walked at their preferred walking speed. The plantar pressure measurements were collected using an rs scan 2 m Hi-End footscan® system (rs scan, Paal, Belgium) with a frequency of 200 Hz and sensor dimensions of 7.62 mm × 5.08 mm. A total of 10 measurements were collected per foot, then spatiotemporally aligned and averaged using STAPP (Booth, Keijsers, Sijbers, & Huysmans, 2018). The average measurement was then upsampled to 3 mm × 3 mm to obtain a correct foot geometry from the pressure plate with anisotropic sensor dimensions. The arch index was then calculated from the peak pressure image (i.e. the image that contains the maximum pressure at each pixel over the time of the footstep) and the corresponding foot was classified as high, normal, or flat arch as described by Cavanagh and Rodgers (1987). Note that the larger the arch index, the flatter the foot.

3.3. Experimental setup

To evaluate our technique, we built a model from 93 healthy individuals with a normal foot arch (186 feet). Individuals in the remaining three groups - high arch, flat foot, and hallux valgus - were used for testing purposes. Each test consisted of taking a 3D foot scan from one of the test groups and comparing it to the shape distribution in the SSM. Given the number of scans in our model, and a 5% tolerance of an incorrect test result, we calculated that a comparison with our SSM should be able to detect effects with a Cohen's d value of 0.24. This result corresponds to effects in the small-to-moderate range ($0.2 < d < 0.5$).

In the case of the two arch height groups, we hypothesized that these groups would show abnormalities in similar areas around the midfoot. In the case of hallux valgus patients, we hypothesized that shape abnormalities would appear around the hallux (i.e. big toe) and corresponding metatarsal. Additionally, we set aside 40 foot scans of healthy individuals with a normal foot arch in order to validate that our technique shows no abnormalities for feet similar to those in the model. A further description of the groups used in model building and testing are shown in Table 2.

4. Results

For each individual's foot, we tested, with FDR correction, how the foot shape deviates from the healthy population. Fig. 4 shows the examples of 6 test subjects (2 subjects per test group) where different regions of shape abnormalities are detected on different subjects. These abnormalities are not only localized in different foot areas for different groups, but the degree of shape abnormality for feet within same group also differs between each other.

In addition, we calculated the outlier histograms to test whether areas of abnormal shape deviations were grouping in specific foot regions for the feet within the same clinical group. At each vertex, we counted the percentage of feet that detected the vertex as a shape outlier. These histograms are shown in Fig. 5. When we tested each foot, we noticed that the outliers were grouping in different foot regions depending on the clinical group to which the foot belongs. For 30% of flat feet, we detected the

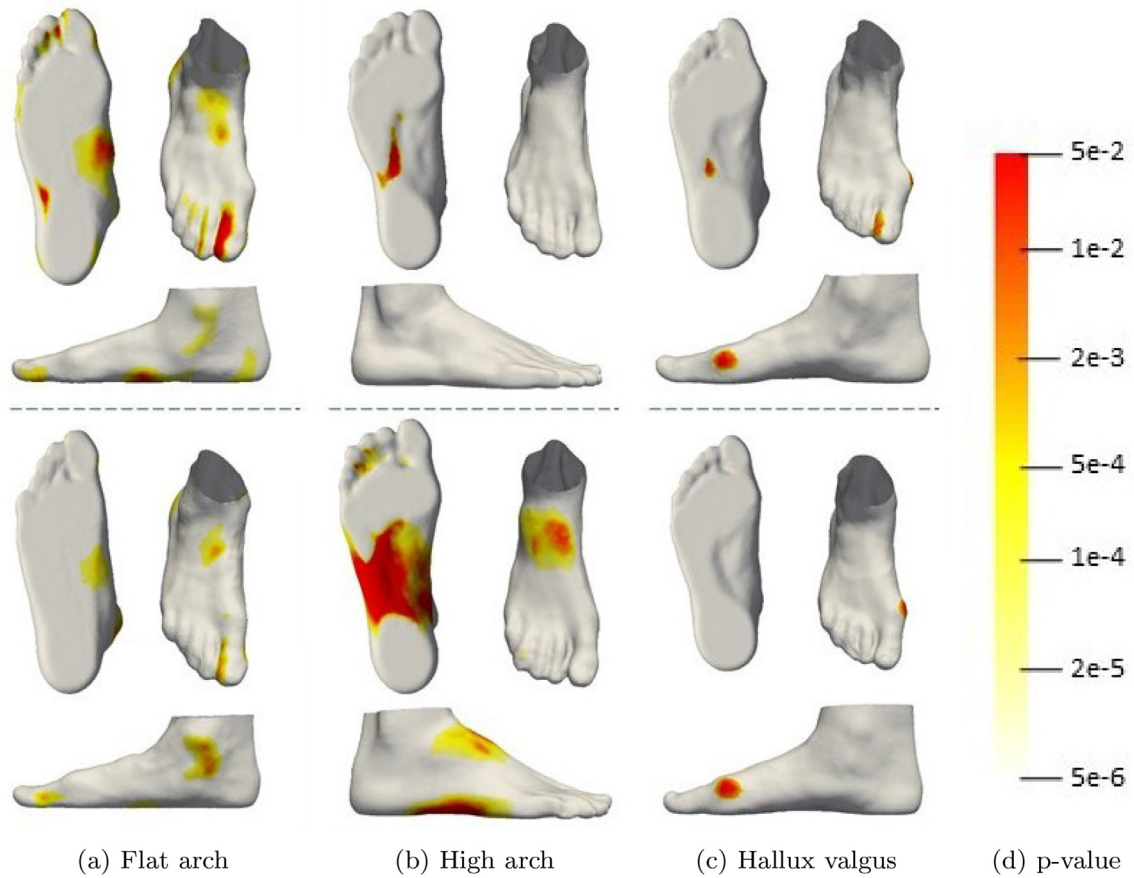


Fig. 4. Example results for 6 individuals within our test groups (2 individuals per group). The detected outlier regions for the 6 test subjects differ not only across groups but also within groups.

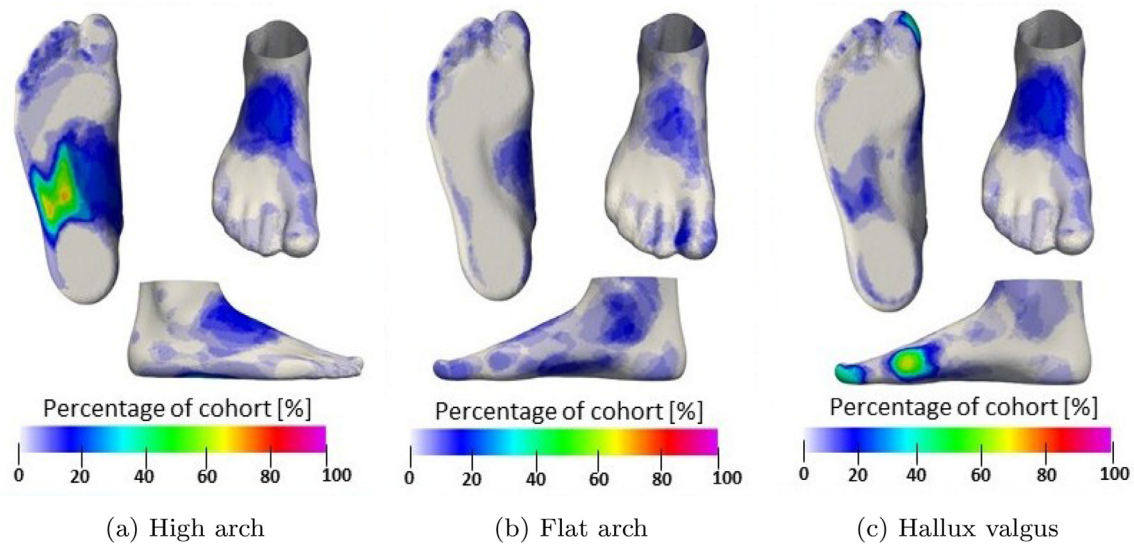


Fig. 5. Histograms of detected outliers ($p < 0.05$) obtained for: a) 40 high arched feet b) 40 flat feet c) 46 feet with hallux valgus.

medial side of plantar midfoot and the upper part of the mid-foot as the main regions of deviation. For 60% of high arched feet, we detected the lateral plantar midfoot as the main region of deviation. For 55% of feet with hallux valgus, we detected the biggest toe and head of the first metatarsal bone as the main regions of deviation, which are expected regions for this deformity. From the normal arched feet we tested, less than 5% showed

outliers and these outliers were not concentrated in any specific region.

For each foot, we measured the size of detected regions and compared them to the clinical measures used to define the groups: arch index and hallux abductus angle (HAA). In experiments performed with high arched and flat arched feet, we did not find a significant correlation between arch indexes and the size of out-

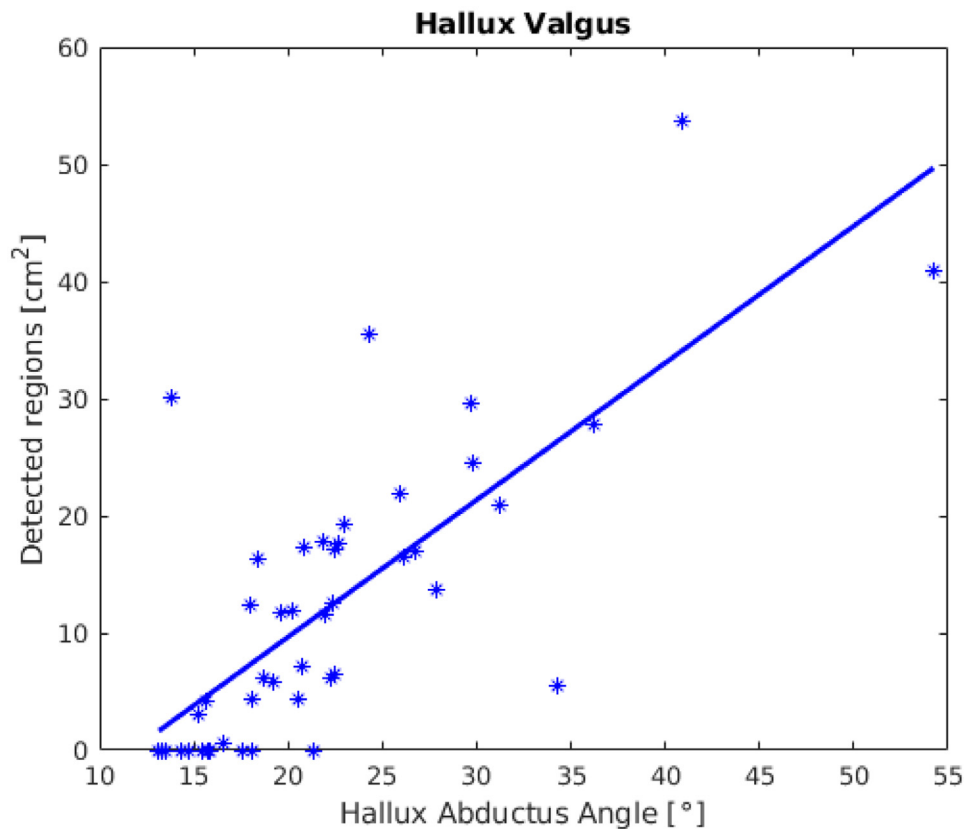


Fig. 6. A significant correlation was found between the size of detected shape abnormalities (in cm²) and the HAA for the feet with hallux valgus ($\rho = 0.76$, $p < 0.001$).

lier regions ($\rho = 0.08$, $p = 0.61$ for flat, $\rho = 0.18$, $p = 0.25$ for high arched). However, we found a significant correlation ($\rho = 0.76$, $p < 0.001$) between HAA and size of the outlier regions for the individuals with hallux valgus feet. Fig. 6 shows the size of the outlier regions within the area of shape deviations typical for hallux valgus deformity.

5. Discussion

We proposed an expert system for objective and personalized identification of 3D foot shape abnormalities through the use of 3D statistical shape modelling. Our system's user interface centered around easy-to-input subject characteristics (e.g. gender, age), allowing for its use by non-experts. Additionally, our system's inference engine relies on established statistical testing procedures, leading to results that are straightforward to interpret. This approach further enables the identification of local regions on the individual's foot that significantly deviate from those of a healthy, normal-arched foot.

Considering arch height variability, we hypothesized that groups with high arched and flat feet would show abnormalities in similar areas around the midfoot. Our results indeed showed significant shape deviations in the midfoot, but interestingly, these shape deviations differed between flat- and high-arched feet. While high-arched feet had outliers concentrated at the lateral plantar midfoot, flat feet showed a decreased concentration of outliers, with abnormalities appearing most prominently at the medial side of the plantar midfoot and at the upper part of the midfoot (Fig. 5). The location of detected regions, along all three dimensions, can be beneficial for footwear manufacturers and can show in which part of the shoe manufacturers should adapt their design to ensure better fitting and more comfortable footwear. For example, the shape deviations found in the plantar midfoot for

high-arched individuals could suggest shoe insoles be adapted to enable more comfortable footwear for this group.

Besides the tests related to arch height, we also tested feet with hallux valgus. We found that the detected shape abnormalities around the hallux and corresponding metatarsal matched our hypothesis. Here, we observed a significant correlation between the hallux abductus angle and the size of the detected regions (Fig. 6). This information can be used to ensure proper footwear width and guarantee that enough space is provided along all three dimensions in the forefoot of a patient's shoe. Given that one of the causes of hallux valgus is poor-fitting footwear, the insights shown by our method could help prevent further development of hallux valgus deformity (Menz & Morris, 2005).

Along with the information on how 3D foot shapes deviate for different groups, our method detected and highlighted whether, and where, the individual's foot deviates from a given healthy population. These personalized foot shape tests showed a variety of abnormal shape regions for the feet within the same clinical group (Fig. 4). This confirms the inter-individual differences found within feet with similar characteristics (Anderson et al., 1956; Debrunner, 1965; Kouchi, 1998). These results are particularly striking given that existing expert systems were used to classify the foot scans analyzed in this study (Cavanagh & Rodgers, 1987; Chen et al., 2013). This indicates that the usual foot examination, based on classifying feet into groups, does not provide a complete picture of foot shape variability. Instead, our method for a personalized and objective analysis of 3D foot shapes shows promise in providing a more complete analysis of foot shape, and analysis that could prove useful for the evaluation of foot deformities.

In comparison to previous expert systems for foot analysis, our approach also employs statistical techniques, thereby increasing the likelihood that foot care professionals will be able to work in

tandem with such a system. In addition, our work expands on existing techniques in two key ways. First, our expert system analyzes the entire 3D foot shape instead of lower-dimensional shape features. This contribution not only simplifies the user interface but also allows the system to produce a more descriptive explanation for why a foot is identified as abnormally shaped. Second, our expert system incorporates demographic measures such as age and weight, measures that allow us to fine tune the inference to a particular individual. Previous systems relied on statistical thresholds that were constant for all individuals, a limitation that impacts the effect sizes that such systems could identify.

At its heart, our proposed foot shape analysis system effectively performs outlier detection, and therefore shares similarities with other outlier detection systems in medicine, economics, data mining, and manufacturing (Domingues, Filippone, Michiardi, & Zouaoui, 2018; Z. Yuan, 2018). Traditionally, outlier detection algorithms have followed one of two approaches. The first, and the one used here, is to build a statistical model of what is considered normal. This model can then be compared to using established statistical tests in order to find outliers (Bazarian et al., 2012; Booth et al., 2016; Stanković et al., 2016). By taking this approach, our system has a strong theoretical foundation for justifying why an exemplar is an outlier (Bouguessa, 2015).

An alternative approach to outlier detection is model-free and seeks to identify outliers based on their similarity to existing data points (Breunig, Kriegel, Ng, & Sander, 2000), specific prototypes (Knorr, Ng, & Tucakov, 2000), or clusters (Duan, Xu, Liu, & Lee, 2009). A strength of these model-free approaches is that they do not require that the data follow a particular statistical distribution, or that a single normative statistical model be considered. Recently, hierarchical approaches have also been proposed for outlier detection in order to achieve this same model-free flexibility (Campello, Moulavi, Zimek, & Sander, 2015). In this work, we have attempted to duplicate this flexibility through a regression between the statistical model and subject demographics. This regression allows us to maintain a strong statistical foundation for our system while also personalizing the model to some degree to the foot under examination.

Overall, our expert system produced results consistent with known foot shape abnormalities while also providing more descriptive and personalized results than previous approaches. Nevertheless, some individuals classified as having an abnormal foot arch or a hallux valgus showed no shape abnormalities in our system (see Figs. 5 and 6). These results suggest that there are limitations to this study or its proposed methods. For example, the 3D scans used in testing were initially classified using the established measures of arch index and hallux abductus angle. Since these measures are an incomplete representation of foot shape, it is possible that feet described as abnormal by those measures may not be statistical outliers when considering the shape as a whole. Additionally, the statistical modelling and regression used in our system also has limitations, specifically that the model assumes the data is normally distributed and that the relationship between foot shape and demographics is linear. These limitations may introduce additional variance into our modelling, thereby reducing its ability to identify foot shape abnormalities. Finally, our choice of demographic features may not be complete. It may be possible to reduce variance in the model if additional information like ethnicity (Razeghi & Batt, 2002), leg dominance (Peters, 1988), and footwear choices (D'Août, Pataky, Clercq, & Aerts, 2009) is included in the regression.

Despite the advantages of our approach to detect outliers in 3D foot shapes, it also has some practical limitations. Detection of 3D foot deviations requires the input of 3D foot scans and, thus, the availability of an optical 3D scanner. The high cost of a quality 3D scanner is a notable disadvantage for our approach over tra-

ditional foot examination methods. The use of existing, cheaper, low-resolution scanners (e.g. Kinect 2, Fuel3D) can be a possible solution. However, our approach would need further evaluation to see if its behaviour changes with the input of lower quality scans. Additionally, the findings presented herein were observed on high resolution scans collected in a standing pose. Many foot deformities have a more noticeable impact on gait than foot shape (Leardini et al., 2007). As a result of this constraint, foot deformities that affect only foot motion are unlikely to be detected using our framework. It is for this reason that we tested individuals who have feet with hallux valgus, a deformity which is visible on static 3D foot scans. Despite this limitation, we showed the possibility of automatic, objective, and personalized detection of the hallux valgus deformity, as well as subtle foot arch deviations present in healthy foot shape.

6. Conclusion

In summary, our expert system for assessing 3D foot shape provides an automatic and objective procedure to examine whether, and where, a single foot shape differs from a healthy foot population. We validated our technique on four groups of feet with different known shape deviations and the results generally matched our hypotheses. However, our analysis technique provided additional insights into how arch height influences foot shape as well as capturing individual variability within each foot group. This information has the potential to be used for various purposes within several biomedical disciplines, including facilitation of more objective clinical diagnosis techniques as well as more accurate footwear design.

6.1. Implications and future work

While our proposed expert system showed promising results, these results also showed that our proposed system would benefit from additional research. First, we observed that the choice of demographics used to fine tune the statistical model can impact the variance within the model and, in turn, its ability to identify abnormalities. It also influences how well the system generalizes to different individuals. Choosing the right demographic features remains an open research question and is effectively the feature selection problem commonly seen in other statistical modelling and machine learning problems (Liu & Motoda, 2007). Second, the statistical modelling used in our system assumes (a) that foot shapes are normally distributed, and (b) that the relationship between demographics and foot shape is a linear one. While our results seem to agree with those assumptions, it remains to be shown whether those assumptions truly hold. Third, the promise seen in our results may be due in part to our use of a high-quality 3D laser scanner to measure foot shape. It is unclear how this measurement quality impacts our expert system.

Based on this study, we clearly see four areas in which future work would be beneficial: feature selection, model flexibility, model sensitivity, and model completeness. With respect to feature selection, it would be beneficial to explore what features - demographic, environmental, or otherwise - impact foot shape. The evaluation and choice of such features would depend not only on their ability to reduce model variance, but also on user privacy and ease-of-use concerns (Golbeck, 2016; Gorgolewski et al., 2017). With respect to model flexibility, conditional generative adversarial networks (Mirza & Osindero, 2014) and permutation testing (Collingridge, 2013) may provide model-free options for the type of outlier detection we perform here. It remains to be seen if such methods can provide the intuitive explanation of their results that an expert system requires.

Additionally, we aim in the future to extend this study to address both model sensitivity and model completeness. With regards to the former point, we intend to evaluate the proposed system on more accessible, but lower quality, 3D optical scanners. Such an extension may require the consideration of mesh denoising (Sun, Rosin, Martin, & Langbein, 2007) or other data enhancement techniques. With regards to the latter point, we further intend to extend this approach to dynamic 4D data (Boppana & Anderson, 2019). Such an extension could give insights into foot abnormalities that are visible only when an individual is moving.

Funding

This work was supported by the Agency for Innovation by Science and Technology in Flanders (IWT-SB 141520). This research is part of the ICON FOOTWORK project (www.imec-int.com/en/what-we-offer/research-portfolio/footwork) and received funding from the European Union's Horizon 2020 research and innovation programme under the Marie Skłodowska-Curie grant agreement no. 746614.

Declaration of Competing Interest

We wish to confirm that there are no known conflicts of interest associated with this publication and there has been no significant financial support for this work that could have influenced its outcome.

Credit authorship contribution statement

Kristina Stanković: Conceptualization, Formal analysis, Investigation, Methodology, Software, Validation, Visualization, Writing - original draft, Writing - review & editing. **Toon Huysmans:** Formal analysis, Funding acquisition, Investigation, Methodology, Project administration, Resources, Supervision, Validation, Writing - review & editing. **Femke Danckaers:** Investigation, Methodology, Writing - review & editing. **Jan Sijbers:** Funding acquisition, Project administration, Resources, Supervision, Writing - review & editing. **Brian G. Booth:** Conceptualization, Formal analysis, Investigation, Methodology, Supervision, Validation, Writing - review & editing.

Acknowledgments

The authors thank Fien Burg, Philippe Vermaelen, and Saartje Duerinck for collecting the data. We would also like to thank the study participants for their significant contributions to this study.

Supplementary material

Supplementary material associated with this article can be found, in the online version, at doi:10.1016/j.eswa.2020.113372.

References

Agarwal, A., & Rastogi, A. (2018). Anthropometric measurements in Ponseti treated clubfeet. *SCIOT-J*, 4(19).

Ahmad, T., Taylor, C., Lanitis, a., & Cootes, T. (1997). Tracking and recognising hand gestures, using statistical shape models. *Image and Vision Computing*, 15(5), 345–352. doi:10.1016/S0262-8856(96)01136-5.

Anderson, M., Blais, M., & Green, W. T. (1956). Growth of the normal foot during childhood and adolescence. Length of the foot and interrelations of foot, stature, and lower extremity as seen in serial records of children between 1–18 years of age. *American Journal of Physical Anthropology*, 14(2), 287–308.

Barton, J., & Lees, A. (1995). Development of a connectionist expert system to identify foot problems based on under-foot pressure patterns. *Clinical Biomechanics*, 10(7), 385–391.

Bazarian, J. J., Zhu, T., Blyth, B., Borrino, A., & Zhong, J. (2012). Subject-specific changes in brain white matter on diffusion tensor imaging after sports-related concussion. *Magnetic Resonance Imaging*, 30(2), 171–180. doi:10.1016/j.mri.2011.10.001.

Booth, B. G., Keijsers, N. L., Sijbers, J., & Huysmans, T. (2018). Stapp: Spatiotemporal analysis of plantar pressure measurements using statistical parametric mapping. *Gait & posture*, 63, 268–275.

Booth, B. G., Miller, S. P., Brown, C. J., Poskitt, K. J., Chau, V., Grunau, R. E., ... Hamarneh, G. (2016). STEAM- statistical template estimation for abnormality mapping: A personalized DTI analysis technique with applications to the screening of preterm infants. *NeuroImage*, 125, 705–723.

Boppana, A., & Anderson, A. P. (2019). Dynamo: Dynamic body shape and motion capture with intel realsense cameras. *Journal of Open Source Software*, 4(41), 1466.

Bouguessa, M. (2015). A practical outlier detection approach for mixed-attribute data. *Expert Systems with Applications*, 42(22), 8637–8649.

Breunig, M. M., Kriegel, H.-P., Ng, R. T., & Sander, J. (2000). LOF: Identifying density-based local outliers. *ACM Sigmoid Record*, 29(2), 93–104.

Campello, R. J., Moulavi, D., Zimek, A., & Sander, J. (2015). Hierarchical density estimates for data clustering, visualization, and outlier detection. *ACM Transactions on Knowledge Discovery from Data (TKDD)*, 10(1).

de Castro, A. P., Rebelatto, J. R., & Aurichio, T. R. (2010). The relationship between foot pain, anthropometric variables and footwear among older people. *Applied Ergonomics*, 41(1), 93–97.

Cavanagh, P. R., Morag, E., Boulton, A. J., Young, M. J., Deffner, K. T., & Pammer, S. E. (1997). The relationship of static foot structure to dynamic foot function. *Journal of Biomechanics*, 30(3), 243–250. doi:10.1016/S0021-9290(96)00136-4.

Cavanagh, P. R., & Rodgers, M. M. (1987). The arch index: A useful measure from footprints. *Journal of Biomechanics*, 20(5), 547–551. doi:10.1016/0021-9290(87)90255-7.

Chen, W., Zhou, J., Hlavacek, P., & Xu, B. (2013). Approach for measuring the angle of hallux valgus. *Indian Journal of Orthopaedics*, 47(3), 278. doi:10.4103/0019-5413.109875.

Collingridge, D. S. (2013). A primer on quantitized data analysis and permutation testing. *Journal of Mixed Methods Research*, 7(1), 81–97.

Costafreda, S. G., Dinov, I. D., Tu, Z., Shi, Y., Liu, C.-Y., Kloszewska, I., ... Vellas, B., et al. (2011). Automated hippocampal shape analysis predicts the onset of dementia in mild cognitive impairment. *NeuroImage*, 56(1), 212–219.

Dahle, L. K., Mueller, M., Delitto, A., & Diamond, J. E. (1991). Visual assessment of foot type and relationship of foot type to lower extremity injury. *Journal of Orthopaedic & Sports Physical Therapy*, 14(2), 70–74. doi:10.2519/jospt.1991.14.2.70.

Danckaers, F., Huysmans, T., Lacko, D., Ledda, A., Verwulgent, S., Van Dongen, S., & Sijbers, J. (2014). Correspondence preserving elastic surface registration with shape model prior. In *Proceedings - international conference on pattern recognition* (pp. 2143–2148). IEEE. doi:10.1109/ICPR.2014.373.

Danckaers, F., Huysmans, T., Lacko, D., & Sijbers, J. (2015). Evaluation of 3d body shape predictions based on features. In *Proceedings of the 6th international conference on 3d body scanning technologies, lugano, Switzerland* (pp. 27–28).

D'Aouit, K., Pataky, T. C., Clercq, D. D., & Aerts, P. (2009). The effects of habitual footwear use: Foot shape and function in native barefoot walkers. *Footwear Science*, 1(2), 81–94.

Dattalo, P. (2013). *Analysis of multiple dependent variables* (pp. 87–108). Oxford Scholarship Online.

Debrunner, H. (1965). Growth and development of the foot. *Ferdinand Enke: Stuttgart*.

Deselnicu, D. C., Vasilescu, A. M., Mihai, A., Purcarea, A. A., & Militaru, G. (2016). New products development through customized design based on customers' needs. part 2: Foot pathology manufacturing parameters. *Procedia Technology*, 22, 1059–1065.

Dobson, J. A., Riddiford-Harland, D. L., Bell, A. F., & Steele, J. R. (2018). Are underground coal miners satisfied with their work boots? *Applied Ergonomics*, 66, 98–104.

Dohi, M., Mochimaru, M., & Kouchi, M. (2001). Foot shape and shoe fitting comfort for elderly japanese women. *The Japanese Journal of Ergonomics*, 37(5), 228–237.

Domingues, R., Filippone, M., Michiardi, P., & Zouaoui, J. (2018). A comparative evaluation of outlier detection algorithms: Experiments and analyses. *Pattern Recognition*, 74, 406–421.

Duan, L., Xu, L., Liu, Y., & Lee, J. (2009). Cluster-based outlier detection. *Annals of Operations Research*, 168(1), 151–168.

Ferrari, V., Jurie, F., & Schmid, C. (2007). Accurate object detection with deformable shape models learnt from images. In *Proceedings of the IEEE computer society conference on computer vision and pattern recognition* (pp. 1–8). IEEE. doi:10.1109/CVPR.2007.383043.

Ferrari, V., Jurie, F., & Schmid, C. (2010). From images to shape models for object detection. *International Journal of Computer Vision*, 87(3), 284–303. doi:10.1007/s11263-009-0270-9.

Freychat, P., Belli, A., Carret, J. P., & Lacour, J. R. (1996). Relationship between rearfoot and forefoot orientation and ground reaction forces during running. *Medicine and Science in Sports and Exercise*, 28(2), 225–232.

Ganesan, B., Luximon, A., Al-Jumaily, A., Balasankar, S. K., & Naik, G. R. (2017). Ponseti method in the management of clubfoot under 2 years of age: A systematic review. *PloS one*, 12(6).

Garrow, A. P., Papageorgiou, A., Silman, A. J., Thomas, E., Jayson, M. I., & Macfarlane, G. J. (2001). The grading of hallux valgus. The Manchester Scale. *Journal of the American Podiatric Medical Association*, 91(2), 74–78.

Garrow, A. P., Silman, A. J., & Macfarlane, G. J. (2004). The cheshire foot pain and disability survey: Apopulation survey assessing prevalence and associations. *Pain*, 110(1), 378–384.

- Glassner, A. (1994). Building vertex normals from an unstructured polygon list. In *Graphics gems* (pp. 60–73). Elsevier.
- Golbeck, J. (2016). User privacy concerns with common data used in recommender systems. In *Proceedings of international conference on social informatics* (pp. 468–480).
- Goonetilleke, R. (1997). Foot sizing beyond the 2-D brannock method. *Annual Journal of IIE (HK)*, 28–31.
- Gorgolewski, K. J., Alfaro-Almagro, F., Auer, T., Bellec, P., Capota, M., & Chakravarty, M. M. (2017). BIDS apps: Improving ease of use, accessibility, and reproducibility of neuroimaging data analysis methods. *PLoS Computational Biology*, 13(3).
- Harris, M. D., Datar, M., Whitaker, R. T., Jurrus, E. R., Peters, C. L., & Anderson, A. E. (2013). Statistical shape modeling of cam femoroacetabular impingement. *Journal of Orthopaedic Research*, 31(10), 1620–1626.
- Hawes, M. R., Sovak, D., Miyashita, M., Kang, S. J., Yoshihuku, Y., & Tanaka, S. (1994). Ethnic differences in forefoot shape and the determination of shoe comfort. In *Ergonomics*: 37 (pp. 187–196). Taylor & Francis. doi:10.1080/00140139408963637.
- Hawke, F., & Burns, J. (2009). Understanding the nature and mechanism of foot pain. *Journal of Foot and Ankle Research*, 2(1).
- Henri, G. (1971). Continuous shading of curved surfaces. *IEEE Transactions on Computers*, 100(6), 623–629. doi:10.1109/T-C.1971.223313.
- Hill, C. L., Gill, T. K., Menz, H. B., & Taylor, A. W. (2008). Prevalence and correlates of foot pain in a population-based study: The north west adelaide health study. *Journal of Foot and Ankle Research*, 1(2).
- Khanduja, V., Baelde, N., Dobbelaere, A., Van Houcke, J., Li, H., Pattyn, C., & Aude-naert, E. A. (2016). Patient-specific assessment of dysmorphism of the femoral head–neck junction: A statistical shape model approach. *The International Journal of Medical Robotics and Computer Assisted Surgery*, 12(4), 765–772.
- Klein, K. F., Hu, J., Reed, M. P., Hoff, C. N., & Rupp, J. D. (2015). Development and validation of statistical models of femur geometry for use with parametric finite element models. *Annals of Biomedical Engineering*, 43(10), 2503–2514.
- Knippels, I., Saey, T., Van den Herrewegen, I., Broeckx, M., Cuppens, K., & Peer-aer, L. (2014). Comparison of biomechanical foot analyses between nine flemish foot-experts. *Journal of Foot and Ankle Research*, 7(1), A45.
- Knorr, E. M., Ng, R. T., & Tucakov, V. (2000). Distance-based outliers: Algorithms and applications. *The International Journal on Very Large Data Bases*, 8(3–4), 237–253.
- Kouchi, M. (1998). Foot dimensions and foot shape: Differences due to growth, generation and ethnic origin. *Anthropological Science*, 106(Supplement), 161–188.
- Leardini, A., Benedetti, M. G., Berti, L., Bettinelli, D., Nativo, R., & Giannini, S. (2007). Rear-foot, mid-foot and fore-foot motion during the stance phase of gait. *Gait and Posture*, 25(3), 453–462. doi:10.1016/j.gaitpost.2006.05.017.
- (2007). In H. Liu, & H. Motoda (Eds.), *Computational methods of feature selection*. CRC Press.
- Mauch, M., Grau, S., Krauss, I., Maiwald, C., & Horstmann, T. (2009). A new approach to children's footwear based on foot type classification. *Ergonomics*, 52(8), 999–1008.
- Menz, H. B., Fotoohabadi, M. R., Wee, E., & Spink, M. J. (2012). Visual categorisation of the arch index: A simplified measure of foot posture in older people. *Journal of Foot and Ankle Research*, 5(1), 10. doi:10.1186/1757-1146-5-10.
- Menz, H. B., & Morris, M. E. (2005). Footwear characteristics and foot problems in older people. *Gerontology*, 51(5), 346–351.
- Mirza, M., & Osindero, S. (2014). Conditional generative adversarial nets. arXiv preprint 1411.1784.
- Mochimaru, M., Kouchi, M., & Dohi, M. (2000). Analysis of 3-D human foot forms using the free form deformation method and its application in grading shoe lasts. *Ergonomics*, 43(9), 1301–1313. doi:10.1080/001401300421752.
- Naser, S. S. A., & Mahdi, A. O. (2016). A proposed expert system for foot diseases diagnosis. *American Journal of Innovative Research and Applied Sciences*, 2(4), 155–168.
- Nigg, B. M., Cole, G. K., & Nachbauer, W. (1993). Effects of arch height of the foot on angular motion of the lower extremities in running. *Journal of Biomechanics*, 26(8), 909–916.
- Nigg, B. M., Nurse, M. A., & Stehanyshyn, D. J. (1999). Shoe inserts and orthotics for sport and physical activities. *Medicine & Science in Sports & Exercise*, 31, S421–S428. doi:10.1097/00005768-199907001-00003.
- Nix, S., Vicenzino, B., Collins, N., & Smith, M. (2012). Characteristics of foot structure and footwear associated with hallux valgus: A systematic review. *Osteoarthritis and cartilage*, 20(10), 1059–1074.
- Peters, M. (1988). Footedness: Asymmetries in foot preference and skill and neuropsychological assessment of foot movement. *Psychological Bulletin*, 103(2), 179.
- Piecha, J. (2000). The neural network conclusion-making system for foot abnormality recognition. In *Proceedings of imacs world congress (pp.1–8)*. Lausanne, Switzerland.
- Piqué-Vidal, C., & Vila, J. (2009). A geometric analysis of hallux valgus: Correlation with clinical assessment of severity. *Journal of Foot and Ankle Research*, 2(15).
- Razeghi, M., & Batt, M. E. (2002). Foot type classification: A critical review of current methods. *Gait & posture*, 15(3), 282–291.
- Redmond, A. C., Crane, Y. Z., & Menz, H. B. (2008). Normative values for the foot posture index. *Journal of Foot and Ankle research*, 1(1), 6.
- Rodrigo, A. S., Goonetilleke, R. S., & Witana, C. P. (2012). Model based foot shape classification using 2D foot outlines. *CAD Computer Aided Design*, 44(1), 48–55. doi:10.1016/j.cad.2011.01.005.
- Sarghie, B., Mihai, A., & Herghilgiu, I. (2016). E-learning application for 3D modelling of custom shoe lasts using templates. In *The international scientific conference elearning and software for education: 3* (p. 553). “Carol I” National Defence University.
- Shen, K.-k., Fripp, J., Mériaudeau, F., Chélat, G., Salvado, O., Bourgeat, P., Initiative, A. D. N., et al. (2012). Detecting global and local hippocampal shape changes in alzheimer's disease using statistical shape models. *NeuroImage*, 59(3), 2155–2166.
- Shlens, J. (2014). A tutorial on principal component analysis. arXiv preprint 1404.1100.
- Song, J., Hillstrom, H. J., Secord, D., & Levitt, J. (1996). Foot type biomechanics. comparison of planus and rectus foot types. *Journal of the American Podiatric Medical Association*, 86(1), 16–23.
- Stanković, K., Booth, B. G., Danckaers, F., Burg, F., Vermaelen, P., Duerinck, S., ... Huysmans, T. (2018). Three-dimensional quantitative analysis of healthy foot shape: A proof of concept study. *Journal of Foot and Ankle Research*, 11(1), 8. doi:10.1186/s13047-018-0251-8.
- Stanković, K., Danckaers, F., Booth, B. G., Burg, F., Duerinck, S., Sijbers, J., & Huysmans, T. (2016). Foot Abnormality Mapping using Statistical Shape Modelling. In *Proceedings of the 7th international conference on 3d body scanning technologies, lugano, switzerland, 30 nov.-1 dec. 2016* (pp. 70–79). doi:10.15221/16.070.
- Stegmann, M. B., & Gomez, D. D. (2002). A brief introduction to statistical shape analysis. *Informatics and mathematical modelling, Technical University of Denmark, DTU*: 15.
- Storey, J. D. (2011). False discovery rate. In *International encyclopedia of statistical science* (pp. 504–508). Springer.
- Sun, X., Rosin, P. L., Martin, R., & Langbein, F. (2007). Fast and effective feature-preserving mesh denoising. *IEEE Transactions on Visualization and Computer Graphics*, 13(5), 925–938.
- Wang, Y., Cao, L., Bai, Z., Reed, M. P., Rupp, J. D., Hoff, C. N., & Hu, J. (2016). A parametric ribcage geometry model accounting for variations among the adult population. *Journal of Biomechanics*, 49(13), 2791–2798.
- Wunderlich, R. E., & Cavanagh, P. R. (1999). External foot shape differences between males and females and among races. In *Pittsburgh: Research paper presented at 23rd annual meeting of the american society of biomechanics, university of pittsburgh, pittsburgh, pa* (pp. 68–69).
- Xiong, S., Goonetilleke, R. S., Witana, C. P., & Lee Au, E. Y. (2008). Modelling foot height and foot shape-related dimensions. *Ergonomics*, 51(8), 1272–1289.
- Xiong, S., Goonetilleke, R. S., Witana, C. P., Weerasinghe, T. W., & Au, E. Y. L. (2010). Foot arch characterization: a review, a new metric, and a comparison. *Journal of the American Podiatric Medical Association*, 100(1), 14–24. 100/1/14 [pii].
- Young, C. C., Niedfeldt, M. W., Morris, G. A., & Eerkes, K. J. (2005). Clinical examination of the foot and ankle. *Primary Care: Clinics in Office Practice*, 32(1), 105–132.
- Yuan, Z., & X. Zhang, S. F. (2018). Hybrid data-driven outlier detection based on neighborhood information entropy and its developmental measures. *Expert Systems with Applications*, 112, 243–257.
- Zhang, J., Gao, Y., Gao, Y., Munsell, B. C., & Shen, D. (2016). Detecting anatomical landmarks for fast alzheimer's disease diagnosis. *IEEE Transactions on Medical Imaging*, 35(12), 2524–2533.